Proceedings World Geothermal Congress 2020+1
Reykjavik, Iceland, April - October 2021

# The Þeistareykir Geothermal Field, NE Iceland: Sub-surface Structural Analysis Based on Borehole Televiewer Imaging

Unnur Þorsteinsdóttir[1], Valdís Guðmundsdóttir[2], Sigurveig Árnadóttir[1], Anett Blischke[1], Bjarni Gautason[1] and Anette Mortensen[3]

[1]Iceland GeoSurvey (ISOR), Rangárvellir, P.O. Box 30, IS-602, Akureyri, Iceland

[2]Iceland GeoSurvey (ISOR), Grensásvegur 9, IS-108, Reykjavík, Iceland

[3]Landsvirkjun, Háaleitisbraut 68, IS-103 Reykjavík, Iceland

E-mail address: unnur.thorsteinsdottir@isor.is

**Keywords:** Þeistareykir, borehole televiewer, stress field, feed zones, permeability distribution

## ABSTRACT

The Þeistareykir geothermal field is located in Northeast Iceland, within the active Þeistareykir volcanic system, one segment of the northern volcanic zone (NVZ). Geothermal field development and studies during the last 10 years have made available a comprehensive dataset of acoustic borehole Televiewer (BHTV) measurements for 9 of the 18 production wells in the area, alongside standard downhole wireline log and cuttings data. These datasets have been analyzed regarding types, distribution and orientation of fractures. Fracture orientation varies considerably in between the wells despite the rather small field size of Þeistareykir. Results from composite geological and geophysical borehole data analysis provide improved structural constraints for sub-surface modelling of the field in comparison to fluid flow. Three distinct fissure and fault trends were observed in the analysis: a dominating NNE-SSW trend at the surface, with a secondary NNW-SSE component, striking parallel to the Tjarnarás Fault zone, and a minor E-W trend observed to the south of the geothermal field. The different orientation of fractures was studied between wells, which provided a base for a division of the field into four sub-areas. Their structural characteristics are discussed and combined with results from spinner logging. One of the sub-areas, located near the Tjarnarás Fault, shows fractures with various strike orientations as well as abnormally high injectivity indices.

## 1. INTRODUCTION

For centuries, Þeistareykir was mainly known for its abundance of sulphur, as it was the main sulphur mine in Iceland (Jónsson, 1945; Þórðarson, 1998). The first geothermal exploration program in Þeistareykir was performed in 1972–1974 (Karlsdóttir, 1974; Grönvold and Karlsdóttir, 1975). In the following years, geological mapping, geochemical analysis from fumaroles and seismic surveys were conducted in the area (Pálmason, 1971; Ward and Björnsson, 1971; Sæmundsson, 1977; Óskarsson, 1984; Ármannsson et al., 1986). In 1981–1984, another geothermal exploration program was carried out, mainly based on surface exploration. Gíslason et al. (1984) did a joint interpretation of gravity studies, geology and resistivity to estimate the lateral extent and behavior of the system. Stable isotope values were also studied in different sections of the field (Darling and Ármannsson, 1989). The geothermal field has been monitored intermittently from 1991 to record its behavior and changes in the system. Based on collected data, the first production well was located (Gautason et al., 2000) and drilled in 2002 (Guðmundsson et al., 2002), and eighteen production wells have been drilled since. Geophysical logging and cutting analysis from the boreholes have provided further information about the geothermal system, e.g. the stratigraphic framework and temperature distribution. Feed zones have been located based on temperature logging and circulation losses, and Guðmundsdóttir et al. (2018) made a revision of size and location of the eight newest wells, based on spinner logging. The revision gave more detailed information about the depth range and injectivity indices of the feed zones.

For a better understanding of the flow paths in the system, studies on structural data are essential along with existing datasets, as they give indications about primary fault/fracture trends or stress field properties within the field. In recent years, nine of the eighteen production wells have been imaged using borehole televiewer (BHTV) imaging. A BHTV wireline probe transmits sonic pulses to the borehole wall, resulting in 360-degree views of amplitude and travel time contrasts along the borehole wall. These signal contrasts allow the interpreter to identify and analyze structural and geological features in the well. This technique has provided a source of subsurface structural information in the geothermal field along with surface structural mapping results (Sæmundsson et al., 2012; Khodayar et al., 2013). The aim of this study is to provide a comprehensive analysis to increase the understanding of the sub-surface structural heterogeneity within the Þeistareykir geothermal field. The study is based on BHTV analysis results interlinked with other borehole data results, specifically permeability indications based on spinner log datasets.

## 2. GEOLOGICAL SETTING

The Þeistareykir volcanic system is the western-most volcanic system in the norther volcanic zone (NVZ) of Iceland (Figure 1). The NVZ is an approximately 200 km long and 50–100 km wide subaerial segment of the NE Atlantic mid-oceanic ridge system and one segment of the onshore Iceland plate boundary, which continues below the Vatnajökull glacier southwards and interlinks with the Tjörnes fracture zone (TFZ) at its northern boundary. The TFZ consists of the Dalvík seismic zone, Húsavík-Flatey transfer zone, and the Grímsey oblique rift system (Sæmundsson, 1974, 1978; Einarsson and Sæmundsson, 1987; Brandsdóttir and Menke, 2008; Einarsson, 2008; Thordarson and Höskuldsson, 2008; Magnúsdóttir et al., 2015; Brandsdóttir et al., 2015; Hjartardóttir et al., 2013, 2016, 2017; Drouin et al., 2017; Hjartarson et al., 2017; Sigmundsson et al., 2018). The structure of this divergent plate boundary is suggested to be spreading faster than average mid-oceanic ridge boundaries, which is reflected by the highly fractured and faulted fissure swarms and their episodic intrusives (Hjartardóttir et al., 2017). Fracture zones, such as the TFZ are known to form normal faults, and local reverse faulting and strike-slip fault segments (Khodayar and Einarsson, 2004; Guðmundsson et al., 2008).

The Þeistareykir fissure swarm is one of the youngest post Pleistocene-Pliocene NVZ regions that consists of 5–6 fissure and central volcanic systems. Those systems have been subdivided and are monitored by seismic activity, surface structural, geological and geothermal expressions (Björnsson et al., 1977; Sigurðsson and Sparks, 1978; Einarsson, 1991). These central volcanic systems are interlinked through their fissure swarms (Sæmundsson et al., 1978) that form overlapping en-echelon domains up to 100 km in length and approximately 20 km in width. During rifting episodes, this pattern changes dramatically, as intensive earthquake activity is felt and measured directly both within the central volcanoes as well as in distinct parts of the linked fissure swarm (see, e.g., (Einarsson and Brandsdóttir, 1980; Buck et al., 2006)). The Þeistareykir fissure swarm extends from Lake Mývatn in the south to Öxarfjörður Bay in the north. The western part of the Þeistareykir fissure swarm, on the one hand, amalgamates with trans-tensional dextral faults of the Húsavík-Flatey-Fault system. The eastern part of the fissure swarm may, on the other hand, intercalate with fissures associated with the offshore Mánáreyjar volcanic system. However, the nature of this transition is debated (Magnúsdóttir and Brandsdóttir, 2011; Sæmundsson, et al., 2012).

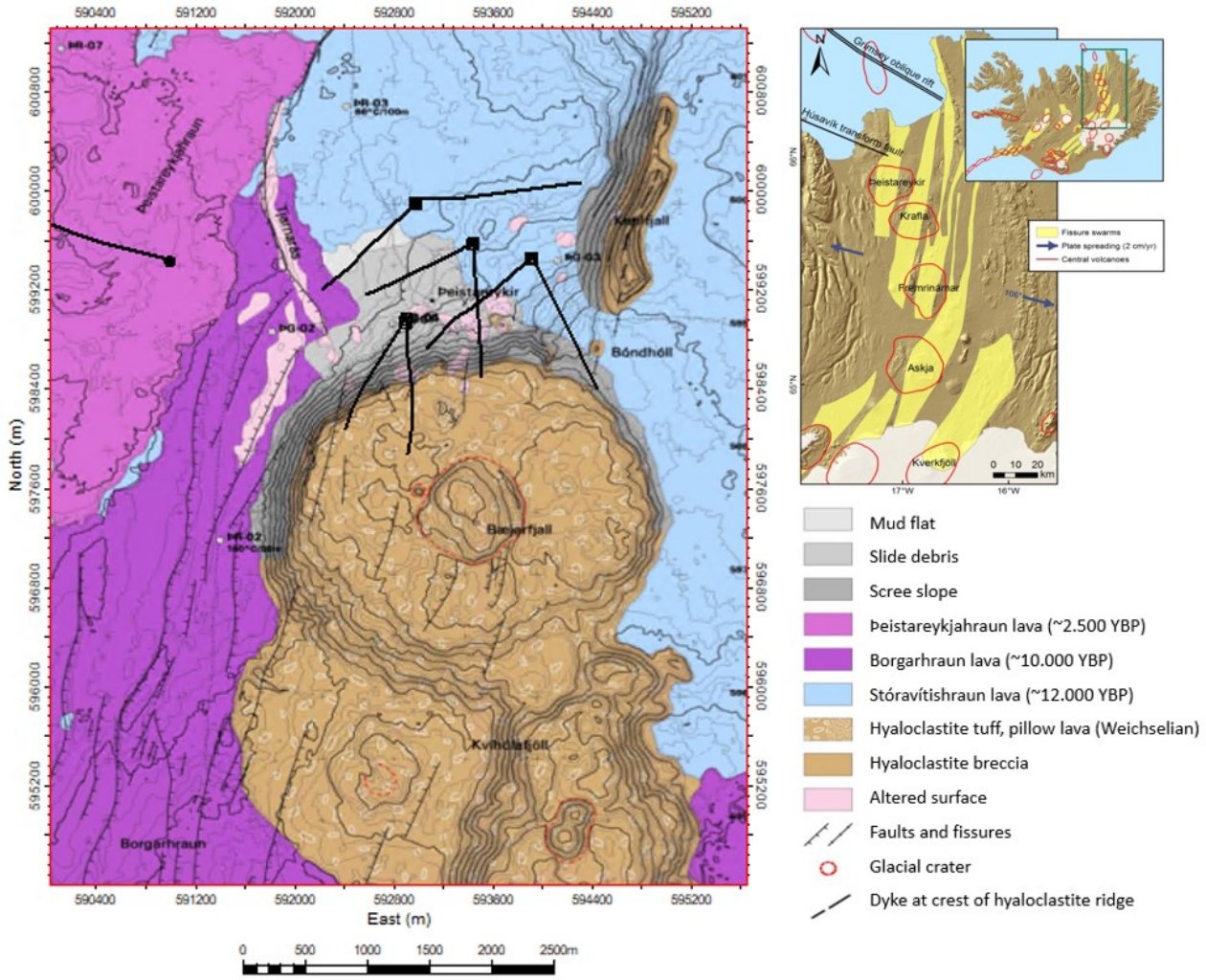


**Figure 1: A geological map showing the main geological formations in the Þeistareykir area. Well paths are shown as black lines. Modified from (Sæmundsson et al., 2012). The location of Þeistareykir is shown on a map modified from (Hjartardóttir et al., 2012).**

As these regional studies increase the understanding for the present-day active part within the NVZ, it is challenging to measure and map these volcanic systems, fissure swarms, and fracture zone systems within a geothermal field scale. The Þeistareykir volcanic system is approximately 70–80 km long and approximately 7–8 km wide in the center, where its width is the greatest. This complex structural and volcanic area is reflected at the surface by a more complex fault and fracture trend system, such as a dominating NNE-SSW general rift and fissure trend, a secondary NNW-SSE trend of the Tjarnarás Fault zone, and a minor W-E trend observed to the south of the geothermal field (Sæmundsson et al., 2012; Khodayar et al., 2013).

Mt. Bæjarfjall is a prominent subglacial hyaloclastite mountain in the central region, formed during the Weischelian time. It is the youngest of the subglacial volcanic formations (Sæmundsson et al., 2012). To the south of Mt. Bæjarfjall, older hyaloclastite mountains are known and referred to as "Kvíhólafjöll". To its north and east, a subglacial ridge was mapped and is referred to as the "Ketilfjall" (kettle mountain) (Figure 1). A prominent volcanic shield "Þeistareykjabunga" is located further east of Ketilfjall, and a distinct crater "Borgarhóll" can be seen to the south and east of Bæjarfjall that produced the lava field "Borgarhraun" (~10000 YBP), which overlays the "Stórahvítishraun" lava field (~12000 YBP). The Þeistareykjahraun lava field (~2500 YBP) is the youngest surface exposed lava field around Mt. Bæjarfjall.

## 3. METHODOLOGY

BHTV analysis has been carried out in nine of the Þeistareykir wells by ÍSOR and GeothermEx (Blischke and Árnadóttir, 2012; Perdana, 2018a, 2018b, 2018c; 2019; Þorsteinsdóttir et al., 2018a, 2018b; Árnadóttir et al., 2018; Helgadóttir et al., 2018). The data were collected from 2011 to 2019 with the ABI-43 (Acoustic Borehole Imaging, 43 mm diameter) logging probe. Data processing and interpretation were performed using Advanced Logic Technology's (ALT) integrated well log interpretation program WellCAD (for wells ÞG-08, ÞG-11, ÞG-13, ÞG-14, ÞG 16) by ÍSOR, and Schlumberger's Techlog wellbore software (for wells ÞG-12, ÞG-15, ÞG-17, ÞG-18) by GeothermEx (Schlumberger). The ABI-43 instrument provides oriented, 360° unwrapped images of the borehole wall by emitting an ultrasonic beam towards the formation and recording the amplitude and the travel-time of the reflected acoustic signal (ALT, 2015). The returning amplitude of the sonic wave relates to the acoustic impedance of the borehole wall, while the travel-time is dependent on the shape and diameter of the well (see, e.g., (ALT, 2015; Davatzes and Hickman, 2010)). Fractures were interpreted manually from the borehole images, recording dip azimuths, dip values and apertures by considering the orientation of the images, and the orientation and caliper of the borehole. The system of fracture classification differs slightly between the two interpretation parties, but in general, fractures were classified into open and closed fractures, and based on their appearance and continuity across the borehole diameter, providing the primary input for the subsurface structural interpretation.

## 4. TELEVIEWER RESULTS

The Þeistareykir wells are primarily drilled as deviated boreholes that reach across most of the 8 km$^2$ large geothermal field. Most wells are located between Mt. Ketilfjall and the Tjarnarás fault, whereas one of the wells; ÞG-08, is located to the west of the Tjarnarás fault, approximately 1.5 km away from the main production area. Depth intervals that were logged using BHTV vary a lot in log image quality. This is due to differences of impedance contrasts within hyaloclastites, washed out or key-hole sections, specifically in highly deviated wells (see, e.g., (Davatzes and Hickman, 2010)). In most wells, only the third drilling phase for the production section of the wells, has been BHTV logged and some wells have only been analyzed over short sections to focus on fractures near large feed zones. The different fracture types have been summarized by their dip azimuth and dip angle for statistical analysis to highlight fault/fracture trends and tie-point with observed inflow zones within the boreholes.

### 4.1 Fracture Orientation

Figure 2 shows the distribution of the dip azimuth of all fractures (+/-90°from the strike). Two primary dip directions are prominent for the area, a dip azimuth range of 85–95°(E) and around 290°(WNW), corresponding to N-S and NNE strike directions. This corresponds to an NNW-SSE to NE-SW strike directional range for fracture elements, with most of the fractures dipping towards WNW and secondary dip direction towards the east. Strike and dip direction variability is apparent in between the wells and field sub-areas (Figure 3). The area furthest to the east, including wells ÞG-18 and ÞG-16, shows a rather homogeneous strike and dip direction, where fractures generally strike NNE-SSW and dip towards WNW. Only short intervals were analyzed for well ÞG-08 in the west, resulting in a slight variation in strike (N-S to NNE-SSW) and a general dip direction towards the east. Similarly, well ÞG-13 shows a regular strike direction from N-S to NNE-SSW with a general dip direction towards the west. Well ÞG-11 appears to have more easterly strike with a dip direction towards SE and NW but not much rotation in fracture strike down the well. Wells ÞG-17 and ÞG-12 show a considerable change and rotation down the borehole, both in strike and dip direction, where the strike ranges from NW-SE to NE-SW. Strike and dip directions vary the most in wells ÞG-14 and ÞG-15, close to the Tjarnarás fault whereas NNW-SSE and E-W striking fractures are present along with NNE-SSW striking fractures. Thus, most irregularities in strike and dip directions are prominent in the western part of the main production area, west and north of Mt. Bæjarfjall (Figure 3).

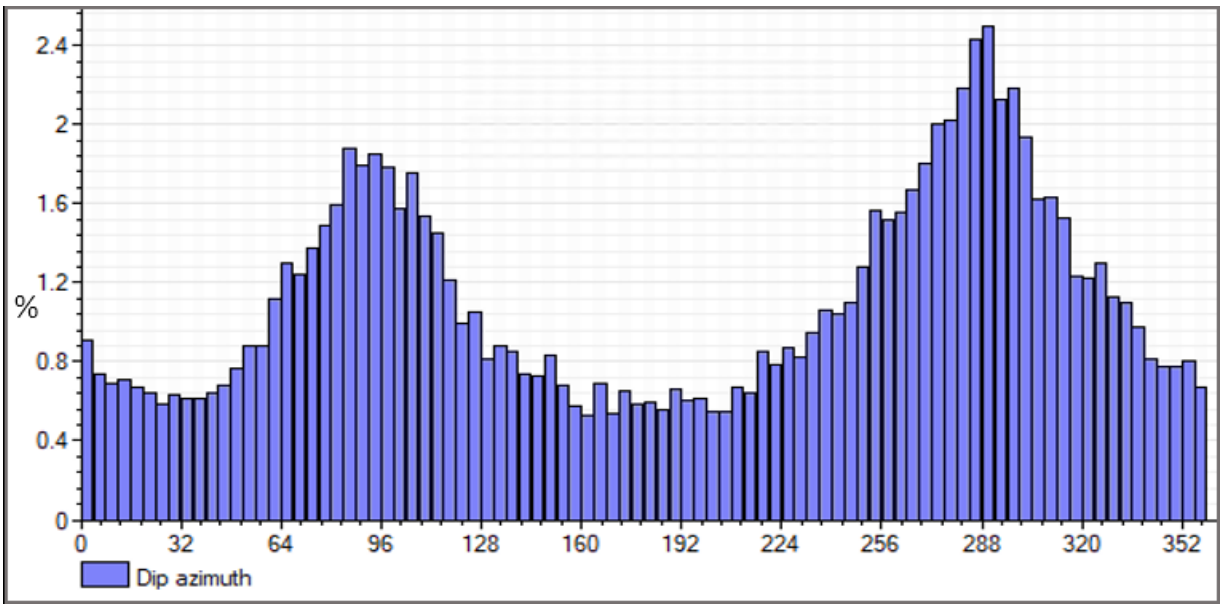


**Figure 2: Dip azimuth histogram display for all interpreted fractures analyzed by ÍSOR and GeothermEx.**

Strike and dip direction of permeable fractures were linked to medium or large feed zones in the wells (Figure 4). Size and locations of feed zones are based on temperature logs, spinner logging and circulation losses, determined at the end of drilling operations. Their orientation is in accordance to the general strike, showing rather homogeneous trend in wells ÞG-08, ÞG-13, ÞG-11, ÞG-16 and ÞG-18, whereas more irregularity is recorded in wells ÞG-17, ÞG-12, ÞG-14 and ÞG-15 within the low area just north of Mt. Bæjarfjall.

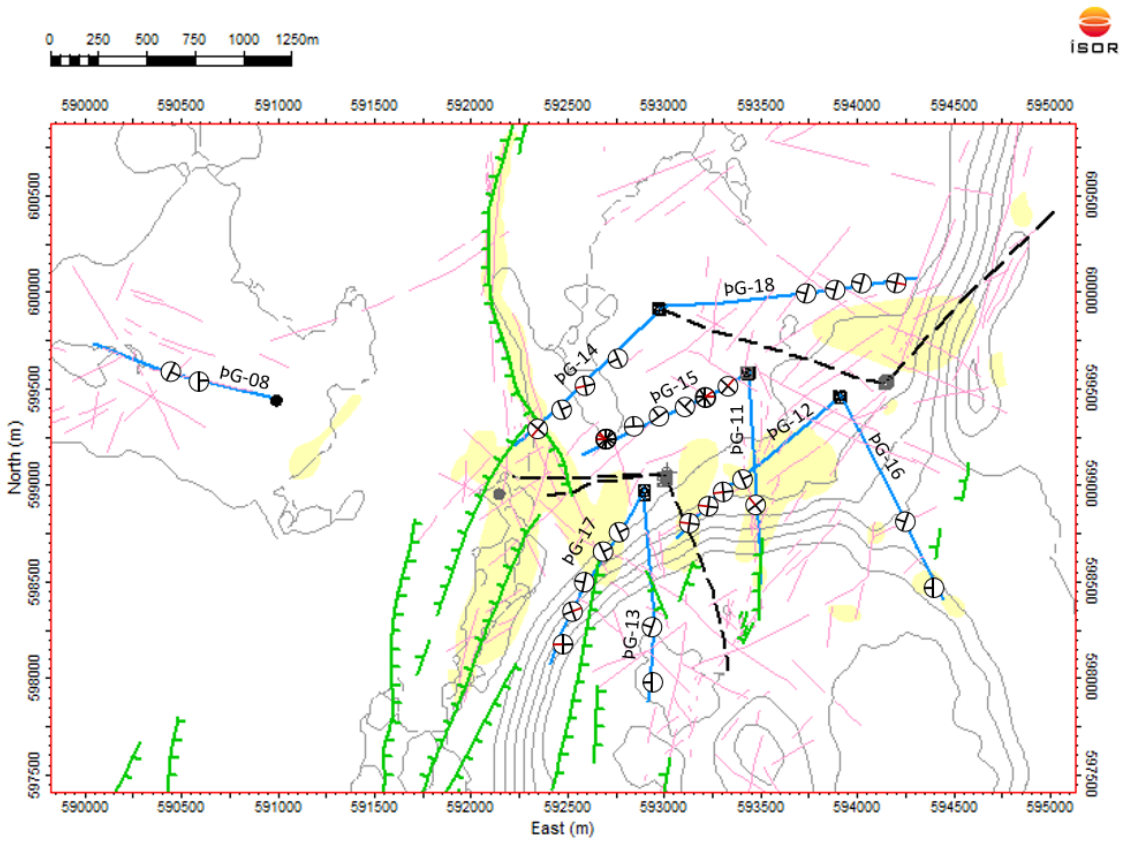


**Figure 3: Circles show the general strike (black long lines in the circle) and dip direction of fractures in all analyzed wells. Black short lines represent the primary dip directions and red short lines represent secondary dip directions. Wells with no BHTV analysis are shown as black dotted lines. The map also shows surface alteration (in yellow), surface fissures and faults mapped by Sæmundsson (2012) in green, and Khodayar (2013) in pink.**

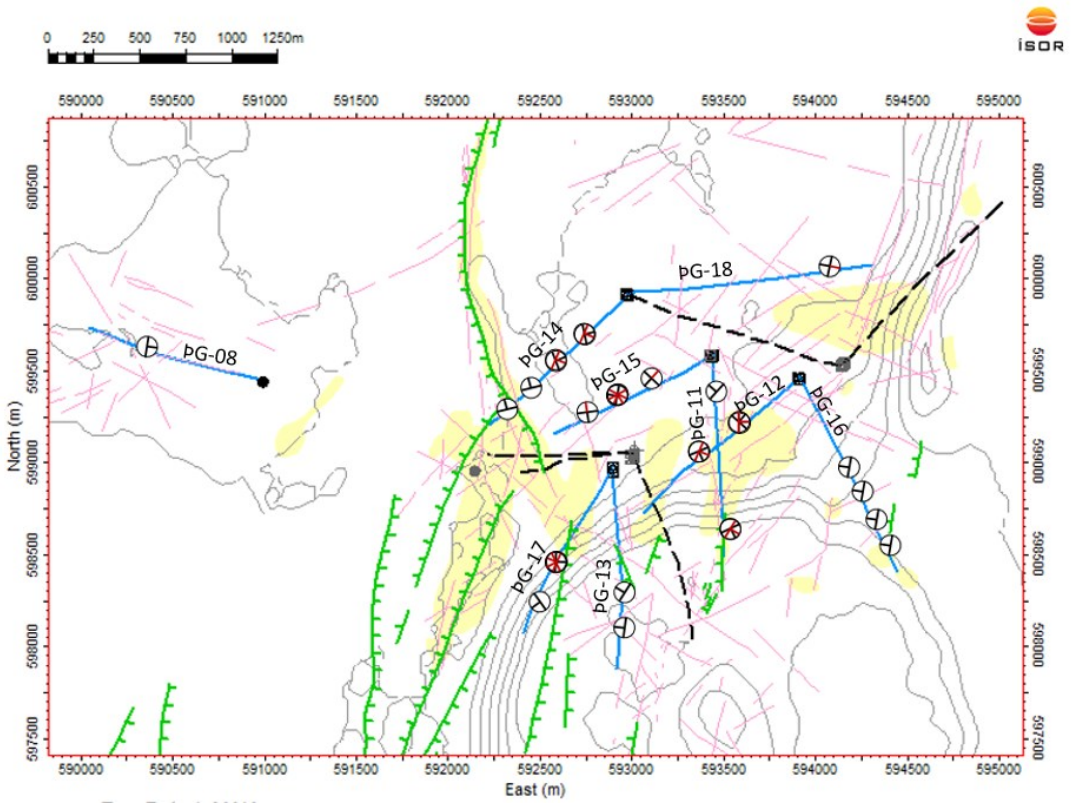


**Figure 4: Strike and dip direction of fractures that are considered to be linked with medium or large feed zones in each analyzed well. Black short lines represent the primary dip directions and red short lines represent secondary dip directions. Wells with no BHTV analysis are shown as black dotted lines. The map also shows surface alteration (in yellow), surface fissures and faults mapped by Sæmundsson (2012) in green, and Khodayar (2013) in pink.**

### 4.2 Orientation of $S_{Hmax}$

Drilling induced fractures (borehole breakouts and drilling induced tensile fractures) have been analyzed in eight of the nine BHTV logged Þeistareykir wells (Figure 5). Borehole ÞG-11 did not have drilling induced fractures analyzed. Borehole breakouts form along the azimuth of the minimum horizontal stress $S_{hmin.}$ and drilling induced tensile fractures occur parallel to the maximum horizontal stress $S_{Hmax.}$ This relationship enables us to assess in which directions fault and fractures are likely to be open and if field areas appear to be segmented or intersecting specific fault zones. As this is applicable for vertical to near vertical boreholes and not necessarily reliable for wells that deviate by more than 10–12° from vertical (e.g.Mastin, 1998, Lacazette 2001 or Ziegler et al., 2016), this analysis is challenging in the Þeistareykir field area, as the wells are primarily deviated and exceed borehole deviation dip values of 10–12° from vertical. Therefore, borehole breakouts and drilling induced tensile fractures are interpreted with caution and may not represent the true orientation of the two horizontal stresses. However, they represent estimated values for the wells. $S_{Hmax}$ strikes nearly N-S for wells ÞG-12, ÞG-13, ÞG-16 and ÞG-18. Well ÞG-15 reflects a NE-SW orientation and ÞG-17 shows a NNW-SSE orientation. Borehole ÞG-14 is the only borehole in the field that records a change in stress field with depth in reference and ties to the Tjarnarás fault intersection below 2000 m in measured depth (MD) (Figure 5).

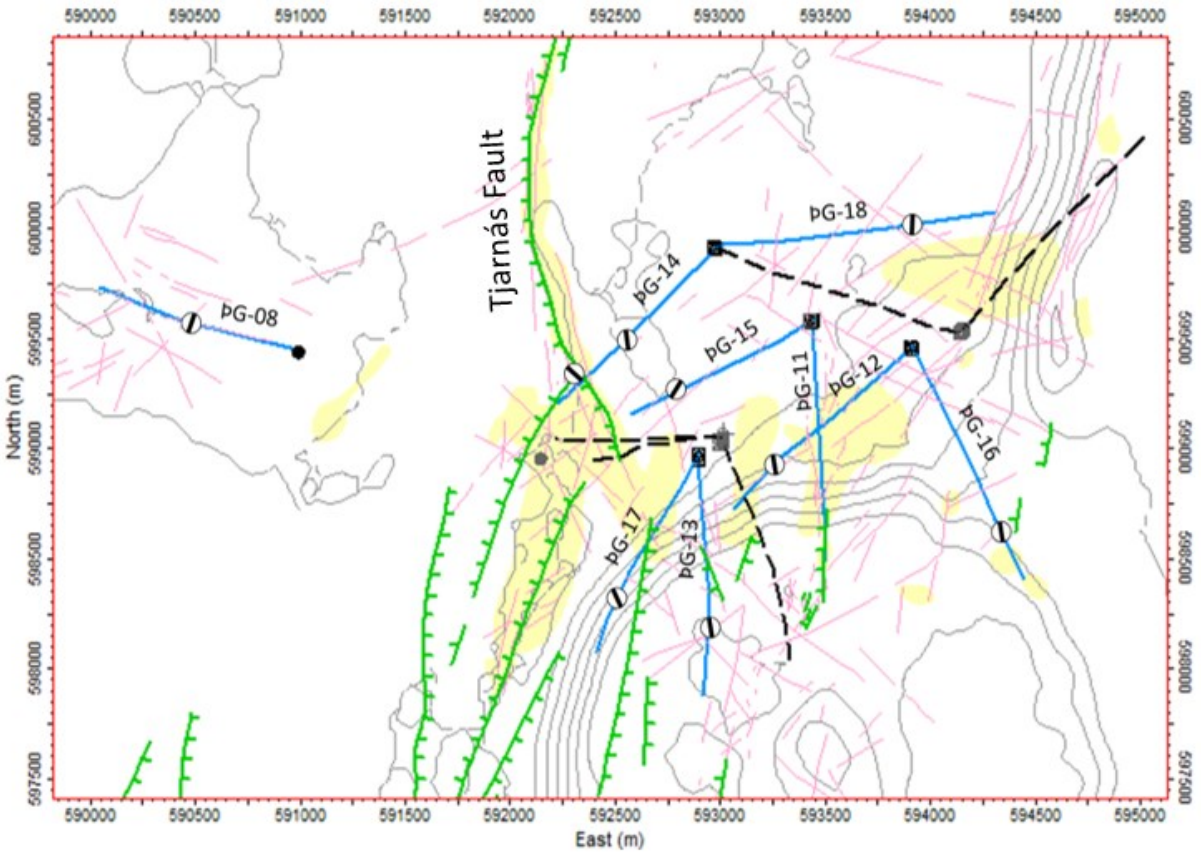


**Figure 5: Directions of $S_{Hmax.}$ analysis for eight of the nine Þeistareykir field wells (black lines). Wells with no BHTV analysis are shown as black dotted lines. The map also shows surface alteration (in yellow), surface fissures and faults mapped by Sæmundsson (2012) in green, and Khodayar (2013) in pink.**

## 5. PERMEABILITY STRUCTURE

Permeability for the Þeistareykir field area was studied and quantified by Guðmundsdóttir et al. (2018) for wells ÞG-11 to ÞG-17, which had enough datasets available. Locations of feed zones were re-evaluated based on spinner log data. Their analysis formed the basis for injectivity index calculations of individual feed zones based on pressure and velocity differences under two different flow conditions. A size and depth revision was presented for feed zones of wells ÞG-12, ÞG-13, ÞG-14, ÞG-15, ÞG-16 and ÞG-17. Figure 6 shows the distribution of injectivity indices. The wells that show the highest injectivity indices are wells ÞG-14 and ÞG-15 (2.59–3.09 (L/s)/bar). Wells ÞG-13, ÞG-17, ÞG-12 and ÞG-16 show medium to minor injectivity indices. This sheds light on the high permeability in wells ÞG-14 and ÞG-15, where fractures have various strike and dip orientations. Total flow from these two wells, as well as from ÞG-13 and ÞG-17 is also rather high (15.33–33.38 kJ/kg). In contrast to the high injectivity indices, wells ÞG-14 and ÞG-15 are recording low enthalpy and electrical power outputs (Guðmundsdóttir et al., 2020). To further the quantitative analysis of the feed zones from Guðmundsdóttir (2018), structural and lithological data was compiled for the feed zones, with the aim of clarifying aspects of the nature of the permeability in Þeistareykir. Wells ÞG-8, ÞG-10 and ÞG-18 were excluded from that analysis due to lack of data.

### 5.1 Permeability in Relation to Feed-Zones and Lithology

Information on the lithological characteristics of the bedrock within each feed-zone interval was added to the existing dataset where available from cuttings: rock type, presence of an intrusion, alteration intensity of the rock, abundance of calcite and pyrite, and level

of vein fillings. Unfortunately, the data coverage on secondary minerals was too sparse to warrant any further investigation. The level of alteration had been classified as high for 76% of the feed zones and medium for 11% of the feed zones. 52% of the feed zones are situated at a great depth, where an intrusions or possible intrusions have been detected. To obtain the dominant fracture orientation and dip value over the depth range of each feed zone, the average of the strike and dip values was calculated as well as their standard deviation. The fractures included in this analysis were the open and the partially open fractures, which had been analyzed with high and medium confidence. All other fractures were omitted.

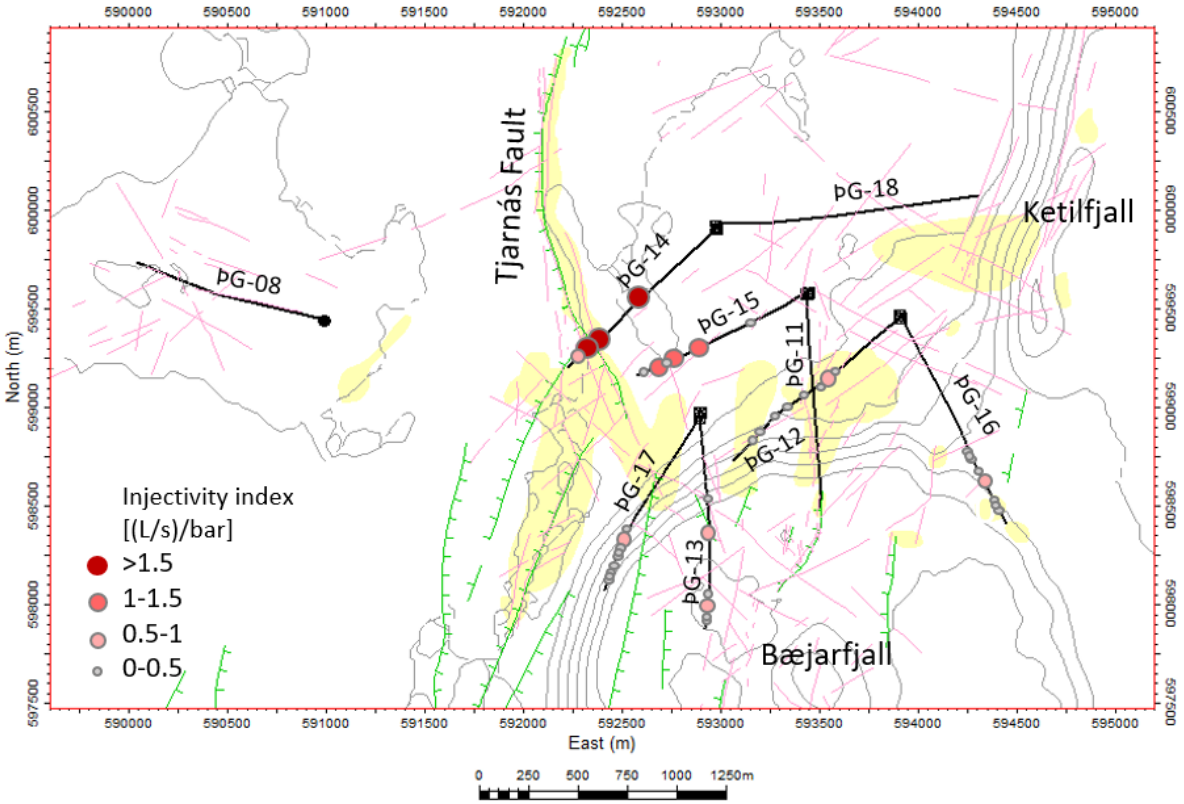


**Figure 6: Feed zone and injectivity index comparison in-between wells, based on spinner log data analysis (Guðmundsdóttir, 2018). The map also shows surface alteration (in yellow), surface fissures and faults mapped by Sæmundsson (2012) in green, and Khodayar (2013) in pink.**

5.1.1 Fracture System

To address the question of what fracture sets of individual feed zones are most permeable in direct comparison to the injectivity index, each feed zone's injectivity index was compared to the mean strike from the BHTV analysis. Fractures striking N-S to NNE-SSW are most common near permeable zones. This may simply reflect the population, since most fractures in the Þeistareykir field are oriented between 0° and 20° and thus reflect the main rift trend. The mean fracture dip value at the depth interval of each feed zone was compared with the feed zone's injectivity index (Figure 7). The most permeable feed zones have dip values between 60° and 72° from horizontal.

5.1.2 Permeability and Depth

Figure 8 shows, on the one hand, how the injectivity index varies with depth (in m.a.s.l.) in the wells and, on the other hand, how the number of feed zones varies with depth in the wells. The permeability increases with depth in the wells and is highest beween 1450 and 1800 m.a.s.l.

5.1.3 Fracture Orientation and Dip with Depth

The mean fracture strike and dip values of the open and partially open fractures located close to feed zones were compared to their depth in m.a.s.l. (Figure 9). The relationship of fracture dip values with depth indicates a slight decrease in dip (fractures dipping more gently deeper in the well) values with depth and a correlation coefficient of 0.28. The strike versus depth shows more northerly striking fractures deeper in the well.

5.1.4 Permeability and Lithology

In order to clarify, which lithological groupings are most associated with permeability in the wells, the feed zones were classified into one of the following categories: basaltic tuff, basaltic breccia, glassy basalt, fine-medium grained basalt, medium-coarse grained basalt, coarse crystalline basalt and intermediate tuff (Figure 10). These categories are obtained from cuttings and therefore intervals in wells where no cuttings were retrieved (due to total loss of circulation) are not included in this analysis. The lithological characteristics most commonly associated with permeability in the wells under study are fine–medium grained basalt and medium–coarse grained basalt that relate to lava flows, dyke or sill intrusions (52% of the permeable fractures are located near intrusions). Furthermore, the highest injectivity indices of individual feed zones were registered in those same two lithological

categories. It is worth noting that in wells Þg-14 and Þg-15 no cuttings were retrieved from below -1075 and -1410 m.a.s.l., respectively. Below these depths gamma logs indicate the presence of intermediate/felsic rocks which have been speculated to be associated with high permeability (Guðjónsdóttir et al., 2017; Sigurgeirsson et al., 2017). In well Þg-14, which has high overall permeability, all the feed zones are situated below the depth of total circulation loss, where no cuttings were retrieved, and are therefore not included in this analysis of permeability and lithology. In Þg-15 two out of the three most permeable feed zones are situated in zones of total loss of circulation.

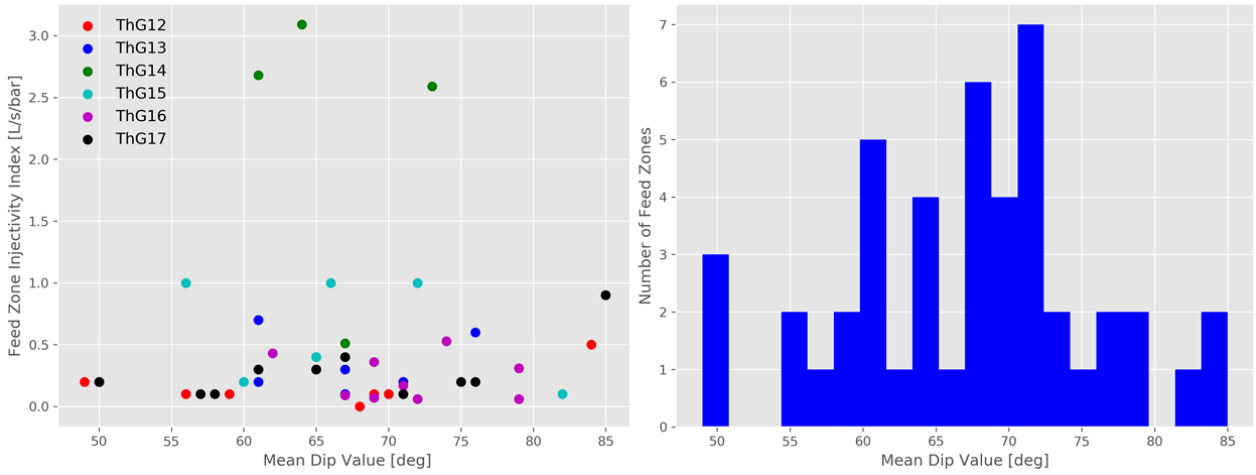


**Figure 7: Left image: The injectivity index of feed zones plotted against the mean dip value of fractures at the depth of each feed zone. Right image: A histogram depicting the number of feed zones per mean dip value.**

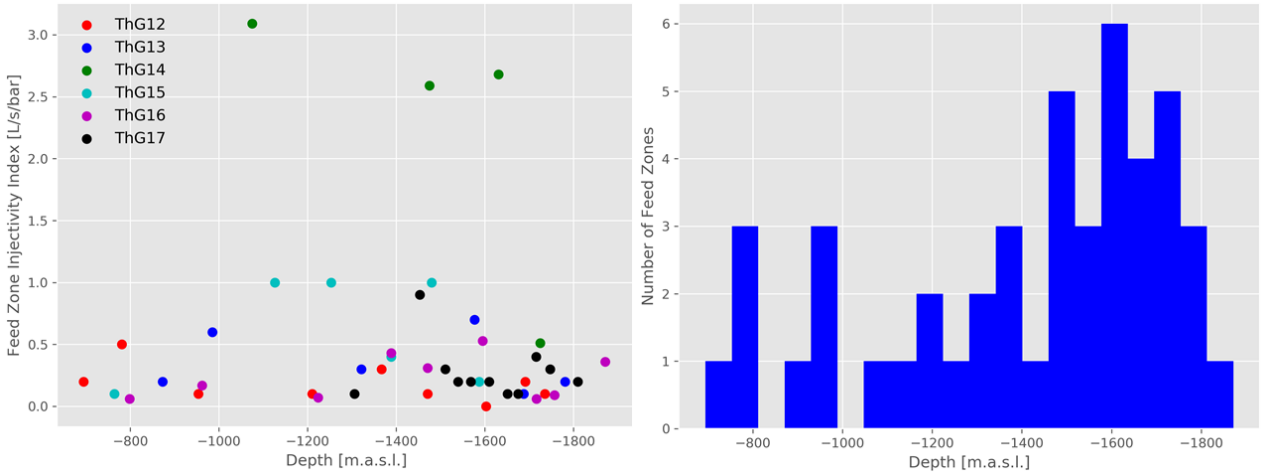


**Figure 8: Left image: The injectivity index of feed zones plotted against the measured depth of each feed zone. Right image: A histogram depicting the number of feed zones per depth interval.**

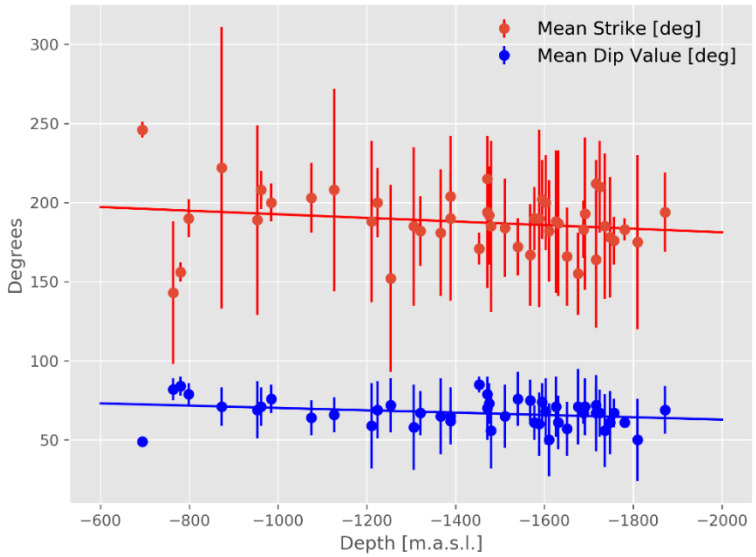


**Figure 9: The mean strike and the mean dip values for the fracture sets around the feed zones are plotted against depth in m.a.s.l. The standard deviation of the strike and dip is plotted in the form of error bars for each feed zone.**

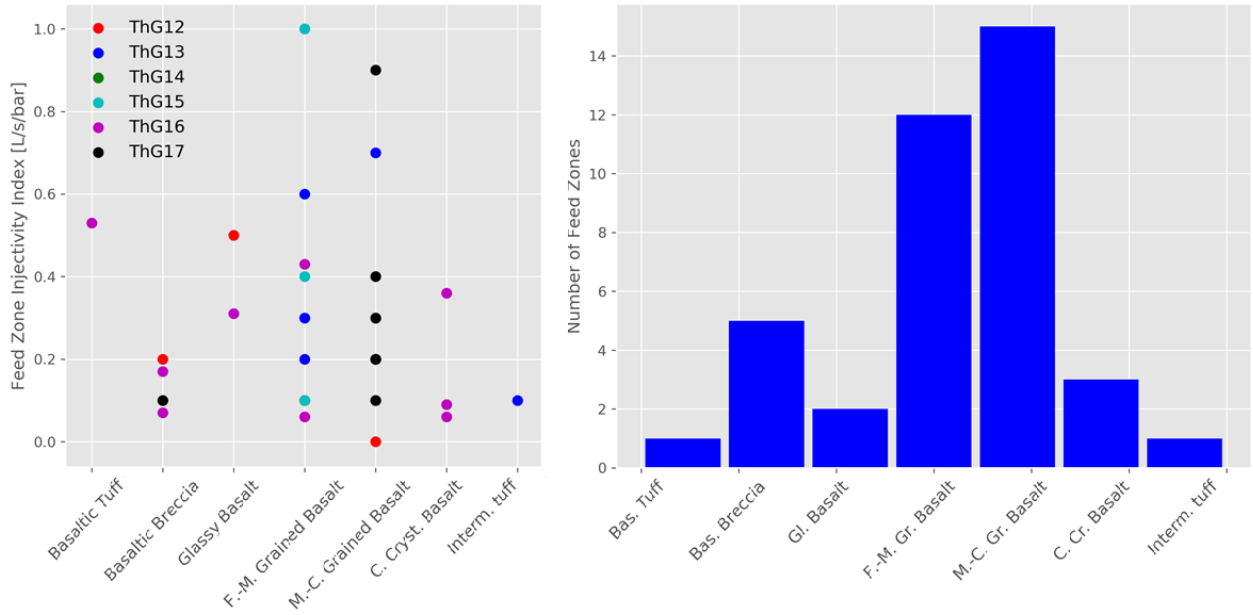


**Figure 10: Left image: The injectivity index of each feed zone plotted against the lithological characteristics of each feed zone. Data from each well is colored differently, no cuttings were retrieved from below 1450 m (MD) where the feed zones are located in ThG-14. Right image: The number of feed zones in each lithological category.**

## 6. DISCUSSION

Based on the difference in BHTV results, the geothermal field can be sub-divided into four sub-areas with the distribution of injectivity indices supporting the grouping (Figure 11). The dip direction of open and partially open fractures, which were analyzed with high or medium confidence, are shown in Figure 12.

Sub-area A: This sub-area reaches from the southern part of the Tjarnarás fault and along the northern flank of Mt. Bæjarfjall. It includes wells ÞG-14 and ÞG-15 and wells ÞG-05, ÞG-05B and ÞG-09, which have not been logged with the BHTV probe. The strike of fractures within this sub-area is highly distributed and the variation in strike, dip and dip direction is considerable within each well. Compared to other sub-areas, mapped surface structural features are few. The Tjarnarás fault system seems to affect the area considerably at depth. The orientation of $S_{Hmax}$ in ÞG-14 changes across that fault system from N-S strike, towards NW strike of $S_{Hmax}$ as it crosses the fault zone. In well ÞG-15 $S_{Hmax}$ is parallel to surface structural features mapped by Khodayar (2013), striking NE-SW. Injectivity indices calculated for wells ÞG-12 to ÞG-17 are highest within this sub-area, which sheds light on the high permeability of this area.

Sub-area B: Wells ÞG-03, ÞG-06 (upper part), ÞG-07, ÞG-16 and ÞG-18 are located within this sub-area. The area is located at the eastern margin of the geothermal field. Only two of the wells within this sub-area have been logged with the BHTV probe (wells ÞG-16 and ÞG-18). They show comparatively homogeneous strike and dip direction (NNE-SSW and a primary dip direction towards WNW), which corresponds well with the strike of mapped fault and fracture zones at surface for the eastern and northern part of this

sub-area. The orientation is striking further to the east than in other sub-areas, and parallel to a dyke that has been mapped at the surface by Sæmundsson (2012) in Ketilfjall (Figure 1). Orientation of $S_{Hmax}$ is N-S in both wells, which is slightly to the west of the main strike of fractures mapped in the wells.

Sub-area C: This sub-area is located in the western flanks of Mt. Bæjarfjall. Wells ÞG-17, ÞG-13, ÞG-12, ÞG-11 and ÞG-04 are located within that area. Fractures show two dominant dip directions; towards E and WNW, which corresponds to N-S and NNE-SSW striking fracture systems. The most heterogeneity in dip directions is recorded within wells ÞG-17 and ÞG-12. The orientation of $S_{Hmax}$ is similar to other sub-areas; striking NNW-SSE.

Sub-area D: This sub-area is located to the west of the main production area and includes only one well, ÞG-08. The BHTV dataset spans only across a short interval of the well indicating a relatively uniform strike of the logged fracture set in a N-S to NNE-SSW direction and a primary dip direction to the east following into the main rift graben low.

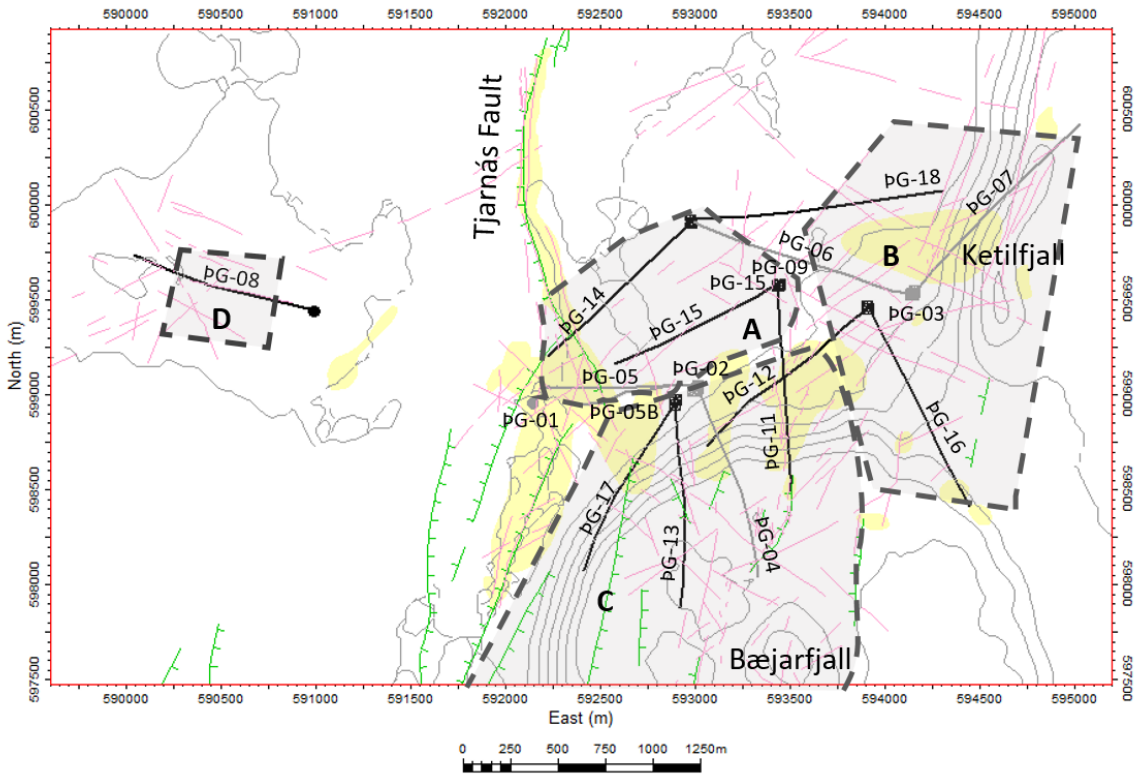


**Figure 11: The four different sub-areas of Þeistareykir, based on results from BHTV analysis. Older wells, that have not been analyzed with BHTV, are marked in gray. The map also shows surface alteration (in yellow), surface fissures and faults mapped by Sæmundsson (2012) in green, and Khodayar (2013) in pink.**

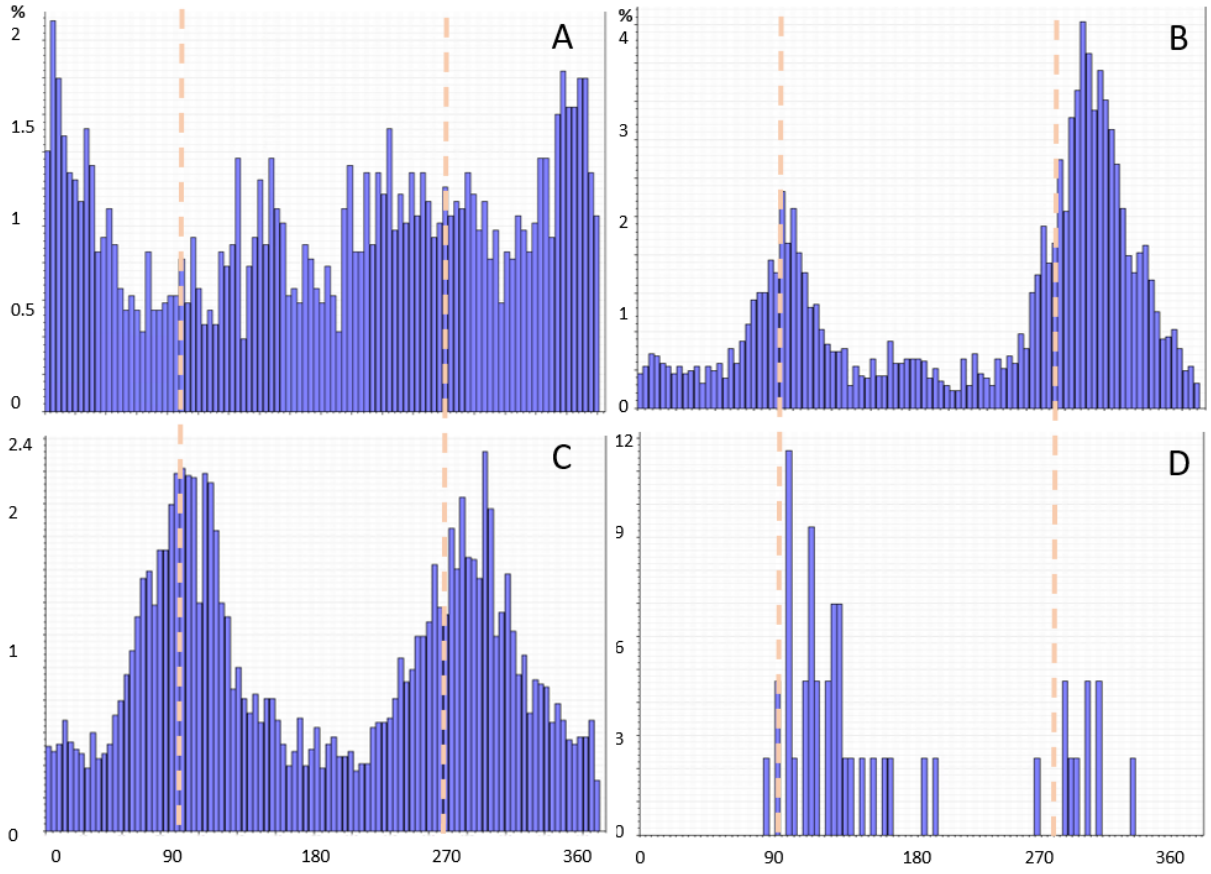


**Figure 12: Dip azimuth in different sub-areas A–D based on BHTV analysis.**

## 7. CONCLUSIONS

The main purpose of the BHTV analysis discussed in this study was to investigate the subsurface fracture network and its control on fluid flow within the Þeistareykir geothermal area. Analysis results are presented for nine of eighteen wells that are distributed over the area. A compilation of the results highlights the structural heterogeneity of the field that sub-divides the field into four distinct structural areas. The heterogeneity exists both between and within wells regarding general fracture strike and regarding fractures that are linked with permeability. One of the sub-areas, including wells ÞG-14 and ÞG-15, shows fractures with various strike orientations as well as abnormally high injectivity indices. Other sub-areas show rather confined fracture strike and dip directions, indicating a dominant NNE-SSW strike direction. Dip direction in the easternmost sub-area B is mostly towards the west, and sub-area D that is located to the west of the main production area and only includes one well indicates a primary dip direction towards the East. Stress orientation measurements show the most common orientation of $S_{Hmax}$ striking N-S, but a westerly rotation of $S_{Hmax}$ is detected in well ÞG-14, which is assumed to be attributed to the Tjarnarás fault zone. In order to clarify aspects of the nature of the permeability, a quantitative analysis was performed of fractures around feed zones with calculated injectivity indices for wells ÞG-12 to ÞG-17. Permeability is highest between 2200 and 2300 m and 52% of fractures near permeable zones are located where an intrusion or a possible intrusion have been detected. Fractures around feed zones strike from NNW to NNE and the most common dip value is between 60° and 72° from horizontal. This study enabled us to tie in detail fracture and feed-zone analysis into a sub-surface fracture network, which is the basis to build a reliable structural field model.

## REFERENCES

Advanced Logic Technology (ALT).: Borehole imaging: Solutions. Viewed 25.11.2016 at ALT‘s website: http://www.alt.lu/borehole.htm (2018).

Ármannsson, H., Gíslason, G., and Torfason, H.: Surface exploration of the Theistareykir high temperature geothermal area, Iceland, with special reference to the application of geochemical methods, *Applied Geochemistry* **1**, (1986), 47-64.

Árnadóttir, S., Tryggvason, H. H., Gunnarsson, B. S., Pétursson, F., Gautason, B., and Blischke, A.: Well ÞG-14. Results of Televiewer Imaging at the Þeistareykir Geothermal Field, NE-Iceland *Iceland GeoSurvey*, technical report, ÍSOR-2018/75 (2018).

Björnsson, A., Sæmundsson, K., Einarsson, P., Tryggvason, E., and Grönvold, K.: Current rifting episodes in North Iceland, *Nature* **266**, (1977), 318-323.

Blischke, A., and Árnadóttir, S.: ÞG-08 Televiewer and Composite Log Data Analysis. ABI-43 Acoustic Borehole Image and Lithology Log Data Provessing and Interpretations for Depth Interval 1493.5-1775 m. *Iceland GeoSurvey*, technical report, ÍSOR-2012/020 (2012).

Brandsdóttir, B., and Menke, W.H.: The seismic structure of Iceland, *Jökull* **58**, (2008), 17-34.

Brandsdóttir B., Hooft, E., Mjelde, R., and Murai, Y.: Origin and evolution of the Kolbeinsey Ridge and Iceland Plateau, N-Atlantic, *Geochemistry, Geophysics, Geosystems* **16**, (2015), 612-634.

Buck, W.R., Einarsson, P., and Brandsdóttir, B.: Tectonic stress and magma chamber size as controls on dike propagation: Constraints from the 1975-1984 Krafla rifting episode, *Journal of Geophysical Research – Solid Earth* **111**, (2006), B12404.

Davatzes, N. C., and Hickman, S. H.: Stress, Fracture, and Fluid-flow Analysis Using Acoustic and Electricial Image Logs in Hot Fractured Granites of the Coso Geothermal Field, California, U.S.A, Í C.-C. a. M. Pöppelreiter, Dipmeter and borehole image log technology, California, *AAPG Memoir* **92**, (2010), 259-293.

Darling, W. G., and Ármannsson, H.: Stable isotopic aspects of fluid flow in the Krafla, Námafjall and Theistareykir geothermal systems of northeast Iceland. *Chemical Geology* **76**, (1989), 197-213.

Drouin, V., Sigmundsson, F., Ófeigsson, B.G., Hreinsdóttir, S., Sturkell, E., and Einarsson, P.: Deformation in the NorthernVolcanic Zone of Iceland 2008–2014: An interplay of tectonic, magmatic, and glacial isostatic deformation, *Journal of Geophysical Research, SolidEarth* **122**, (2017), 3158–3178.

Einarsson, P., and Brandsdóttir, B.: Seismological evidence for lateral magma intrusion during the July 1978 deflation of the Krafla volcano in NE Iceland, *Journal of Geophysics* **47**, (1980), 160-165.

Einarsson, P., and Sæmundsson, K.: Earthquake epicenters 1982–1985 and volcanic systems in Iceland, map, In: Sigfússon, Th. (Ed.), Í hlutarins edli, Festschrift for Thorbjörn Sigurgeirsson, *Menningarsjóður, Iceland* (1987).

Einarsson, P.: Earthquakes and present-day tectonism in Iceland. *Tectonophysics* **189**, (1991), 261-279.

Einarsson, P.: Plate boundaries, rifts and transforms in Iceland, *Jökull* **58**, (2008), 35–58.

Gautason, B., Ármannsson, H., Árnason, K., Saemundsson, K., Flóvenz, Ó.G., and Thórhallsson, S.: Thoughts on the next steps in the exploration of the Þeistareykir geothermal area *National Energy Authority,* technical report BG-HÁ-KÁ-KS-ÓGF-STh-2000/04 (2000).

Grönvold, K., and Karlsdóttir, R.: Þeistareykir – Áfangaskýrsla um yfirborðsrannsóknir jarðhitasvæðisins. *National Energy Authority*, technical report, JHD 7501 (1975).

Guðjónsdóttir, S. R., Guðmundsdóttir, V., Sigurgeirsson, M. Á., Ásgeirsdóttir, R. S., Tryggvason, H. H., Stefánsson, H. Ö., Ingólfsson, H., Pétursson, F., and Gunnarsson, B. S. (2017). Þeistareykir-Well ÞG-14. Phase 3: Drilling for a 7“ Perforated liner down to 2500 m. *Iceland GeoSurvey,* report, ÍSOR-2017/023, 95 pp.

Guðmundsdóttir, V., Þorgilsson, G., and Egilson, Þ.: Spinner Log Processing and Permeability Distribution in the Þeistareykir Geothermal Reservoir, *Iceland GeoSurvey*, technical report, ÍSOR-2018/084 (2018).

Guðmundsdóttir, V., Þorgilsson, G., Júlíusson, E., and Egilson, Þ.: Evaluation and comparison of injection and production indices of feed zones and wells obtained from spinner logs measured during injection and production testing *Proceedings World Geothermal Congress, Reykjavík*, Iceland (2020).

Guðmundsson, Á., Gautason, B., Thordarson, S., Egilson, Þ., and Þórisson, S.: Rannsóknarborun á Þeistareykjum. Hola ÞG-1. 3. áfangi: Borun vinnsluhluta í 1953 m dýpi. Orkustofnun. OS-2002/079 (2002).

Guðmundsson, Á., Friese, N., Galindo, I., and Philipp, S.L.: Dike-induced reverse faulting in a graben, *Geology* **36**, (2008), 123-126.

Helgadóttir, H. M., Árnadóttir, S., Blischke, A.: Þeistareykir – Well ÞG-11. Corrections of previous borehole televiewer log interpretations. *Iceland GeoSurvey,* short report, ÍSOR-18001 (2018).

Hjartardóttir, Á.R., and Einarsson, P.: Sprungusveimar Norðurgosbeltisins og umbrotin í Bárðarbungu 2014–2015 (in Icelandic), *Náttúrufræðingurinn*, **87**, Issue 1-2, (2017), 24-39.

Hjartardóttir, Á.R., Einarsson, P., Magnúsdóttir, S., Björnsdóttir, Þ., and Brandsdóttir, B.: Fracture systems of the Northern Volcanic Rift Zone, Iceland - an onshore part of the Mid-Atlantic plate boundary, In: Wright, T.J., Ayele, A., Ferguson, D.J., Kidane, T., Vye-Brown, C. (Eds.), Magmatic Rifting and Active Volcanism, *The Geological Society of London,* (2016), 297-314.

Hjartardóttir, Á.R.: Fissure swarms of the Northern Volcanic Rift Zone, Iceland, PhD dissertation, Faculty of Earth Sciences, University of Iceland, (2013).

Hjartardottir, Á.R., Einarsson, P, Bramham, E., and Wright, T.: The Krafla fissure swarm, Iceland, and its formation by rifting events, Bull Volcanol, (2012), **74**, 2139-2153.

Hjartarson, A., Erlendsson, Ö., and Blischke, A.: The Greenland–Iceland–Faroe Ridge Complex, In: Péron-Pinvidic, G., Hopper, J.R., Stoker, M.S., Gaina, C., Doornenbal, J.C., Funck, T. and Árting, U.E. (eds), The NE Atlantic Region: A Reappraisal of Crustal Structure, Tectonostratigraphy and Magmatic Evolution, *Geological Society, London, Special Publications* **447**, (2017), 22 p.

Jónsson, Ó. In: Ódáðahraun I-III.: Akureyri, Norðri Book Publisher (1945), pp. 425, 447 and 405.

Karlsdóttir, R.: Forundersögelse af Þeistareykir-området, *Danmarks Tekniske Højskole*, Thesis in Technical Geology, B710905 (1974).

Khodayar, M., and Einarsson, P.: Reverse-slip structures at oceanic diverging plate boundaries and their kinematic origin: data from Tertiary crust of west and south Iceland, *Journal of Structure Geology* **26**, (2004), 1945-1960.

Khodayar, M., and Bjornsson, S.: Preliminary Fracture Analysis of Þeistareykir Geothermal Field and Surroundings, Northern Rift Zone and Tjornes Fracture Zone. *Iceland GeoSurvey,* technical report, ÍSOR-2013/029 (2013).

Lacazette, A.: Natural Fracture Nomenclature, Disk 1, in L.B. Thompson (ed) Atlas of Borehole Images, AAPG Datapages Discovery Series 4, American Association of Petroleum Geologist, Tulsa (2 compact disks).

Mastin, L. Effect of Borehole Deviation on Breakout Orientations. Journal of Geophysical Research, **93**, (1988), 9187-9195.

Magnúsdóttir, S., and Brandsdóttir,B.: Tectonics of the Þeistareykir fissure swarm, *Jökull* **61**, (2011), 65-79.

Magnúsdóttir, S, Brandsdóttir, B., Driscoll, N., and Detrick, R.: Postglacial tectonic activity within the Skjálfandadjúp Basin, Tjörnes Fracture Zone, offshore Northern Iceland, based on high resolution seismic stratigraphy, *Marine Geology* **367**, (2015), 159–170.

Óskarsson, N.: Monitoring of fumarole discharge during the 1975-1982 rifting in the Krafla volcanic center, North-Iceland. *J. Volcanol. Geotherm. Res*, **10**, (1984) 93-111.

Pálmason, G.: Crustal structure of Iceland from explosion seismology. *Soc. Sci Islandica 40,* Phd dissertation, (1971).

Perdana, T. S. P.: ABI Image Processing and Interpretation of Well ÞG-17, Þeistareykir Field, Þingeyjarsveit, Iceland. *Prepared by GeothermEx for the National Power Company of Iceland,* technical report, LV-2018-068 (2018a).

Perdana, T. S. P.: ABI Image Processing and Interpretation of Well ÞG-15, Þeistareykir Field, Þingeyjarsveit, Iceland. *Prepared by GeothermEx for the National Power Company of Iceland,* technical report, LV-2018-069 (2018b).

Perdana, T. S. P.: ABI Image Processing and Interpretation of Well ÞG-15, Þeistareykir Field, Þingeyjarsveit, Iceland. *Prepared by GeothermEx for the National Power Company of Iceland,* technical report, LV-2018-023 (2018c).

Perdana, T. S. P.: ABI Image Processing and Interpretation of Well ÞG-18, Þeistareykir Field, Þingeyjarsveit, Iceland. *Prepared by GeothermEx for the National Power Company of Iceland,* technical report, LV-2019-004 (2019).

Sigmundsson, F., Einarsson, P., Hjartardóttir, Á.R., Drouin, V., Jónsdóttir, K., Árnadóttir, T., Geirsson, H., Hreinsdóttir, S., Lia, S., and Ófeigsson, B.G.: Geodynamics of Iceland and the signatures of plate spreading, *Journal of Volcanology and Geothermal*.

Sigurðsson, H., and Sparks, S.R.J.: Rifting episode in North Iceland in 1874-1875 and the eruptions of Askja and Sveinagja, *Bulletin of Volcanology* **41**, (1978), 149-167.

Sigurgeirsson. M. Á., Guðjónsdóttir, S. R., Ásgeirsdóttir, R. S., Tryggvason, H. T., Egilson, Þ., Guðmundsdóttir, V., Gunnarsson, B. S., Vilhjálmsson, S., Ingimarsson, H., Pétursson, F., and Ingólfsson, H. (2017). Þeistareykir – Well ÞG-15. Phase 3: Drilling for a 7" Perforated Liner down to 2260 m, *Iceland GeoSurvey*, report, ÍSOR-2017/036, 165 pp.

Sæmundsson, K.: Evolution of the axial rifting zone in northern Iceland and the Tjörnes fracture zone, Geological Society of America, *Bulletin* **85**, (1974), 495–504.

Sæmundsson, K.: Geological map, North-East Iceland, 1:250 000. *Icelandic Institute of Natural History and National Land Survey of Iceland* (1977).

Sæmundsson, K.: Fissure swarms and central volcanoes of the neovolcanic zones in Iceland, In: Crustal evolution in northwestern Britain and adjacent regions, Bowes, D.R. and Leake, B.E. (editors), Reprinted from *Geological Journal Special Issue* **10**, (1978), 415-432.

Sæmundsson, K., Magnús, Sigurgeirsson, M.Á, and Grönvold, K.: Þeistareykir: Jarðfræðirannsóknir 2011, *Iceland GeoSurvey,* technical report, ÍSOR-2012/024, (2012).

Thordarson, T., and Höskuldsson, A.: Postglacial volcanism in Iceland. *Jökull* **58**, (2008).

Ward, P.L., and Björnsson, S.: Microearthquakes, swarms and the geothermal areas of Iceland. *J. Geophys. Res*., **76**, (1971), 3953-3982.

Ziegler, M., Heidbach, O., Rajabi, M., Hersir, G.P., Ágústsson, K., Árnadóttir, S., and Zang, A.: The stress pattern of Iceland, *Tectonophysics,* **674**, (2016), 101-1133.

Þorsteinsdóttir, U., Árnadóttir, S., Gautason., Gunnarsson, B.S., Pétursson, F., Ingimarsson, H., and Egilson, Þ.: Well ÞG-16 – Results of Televiewer Imaging at the Þeistareykir Geothermal Field, NE-Iceland. *Iceland GeoSurvey*, technical report, ÍSOR-2018/076 (2018a).

Þorsteinsdóttir, U., Blischke, A, Árnadóttir, S, and Guðmundsdóttir, V.: Þeistareykir – Well ÞG-13. Borehole Televiewer Log Analysis. *Iceland GeoSurvey*, ÍSOR – 2018/045 (2018b).

Þórðarson, S.: Auður úr iðrum jarðar. Saga hitaveitna og jarðhitanýtingar á Íslandi. Safn til iðnsögu Íslands, XII. Hið íslenska bókmenntafélag, Reykjavík. 656 pp (1998).